

MODEL SIMULATIONS OF BAR EVOLUTION IN A LARGE SCALE LABORATORY BEACH

P. Teran Cobo¹, J. T. Kirby¹, M. C. Haller², H. T. Ozkan-Haller³, J. Magallen², G. Guannel³

The current paper reports a test of a coupled Boussinesq/bottom boundary layer model for cross-shore transport, applied under accretional wave conditions. Measurements of free surface elevation, fluid velocities and beach profile evolution were obtained during the CROSSTEX experiment carried out in summer 2005. The model calculations are conducted in predictive mode in order to assess model skill in performing short term assessments of beach profile evolution for single storm events. Fifty twenty-minute long simulations are carried out consecutively, spanning the duration of an accretional event. Strong discrepancies such bar height overprediction arise due to various factors, of which the most significant is the wave reflection on the 1/20 beach slope.

INTRODUCTION

Cross-shore sediment transport processes on simple longshore uniform beaches result from a complex superposition of two and three-dimensional hydrodynamic patterns. Storms produce energetic sea states with waves that break and create turbulence that suspends large amounts of sediment. Under highly energetic storm conditions, breaking waves force near bottom steady flows, also called undertow (Dally and Dean, 1984; Sallenger and Howd, 1989). The equilibrium beach profile will change due to gradients in offshore transport induced by cross-shore undertow, rapidly creating an offshore sandbar. In the presence of a sand bar, wave breaking is enhanced near the bar crest, and reduced near the bar trough (Lippman et al., 1996). Also, bar-intensified undertow has been observed (Sallenger and Howd, 1989; Haines and Sallenger, 1994), with a maximum just shoreward the bar crest (Gallagher et al., 1998).

The dominant role of the undertow during erosional events in energetic surf zones allows models based on quasi-steady hydrodynamics to provide successful predictions of profile erosion and offshore bar migration. Such energetic type sediment transport models (based on Bagnold, Bowen and Bailard equations) were driven with near bottom velocities to predict the offshore migration event observed during the DELILAH 90 experiment (Thornton and Birkemeier, 1996). Further study supports and improves offshore migration prediction based on DUCK 94 experiment measured near bottom velocities (Gallagher et al., 1998). However, wave-averaged transport predictions based on Bagnold or other steady state models (in which fluid acceleration or pressure gradient do not play a significant

¹ Center for Applied Coastal Research, University of Delaware, Newark, DE, 19716, USA

² Dept. of Civil and Construction Engineering, Oregon State University, Corvallis, OR 97331 USA

³ College of Oceanic and Atmospheric Sciences, Oregon State University, Corvallis OR 97331 USA

role) typically fail to predict observed onshore transport or bar migration when used with coefficients similar to those employed in successful offshore transport simulations (Gallagher et al, 1998).

In accretional regimes, shoreward bar migration is observed under milder energetic conditions (Aubrey, 1979) and relatively weak undertow. Outside the surfzone, the wave signal becomes relatively more significant. As waves travel shorewards and shoal, the skewed profiles evolve to asymmetric, with steep and pitched forward front faces (Elgar et al., 1988). The contribution of the onshore skewed velocities may be important outside the surfzone (Trowbridge and Young, 1989), due to the larger onshore velocities under the peaked wave crests than the offshore velocities under the troughs (Bowen, 1980; Bailard, 1981). However, models based on velocity skewness fail to predict onshore bar migration. In the surfzone, under breaking waves, orbital velocity asymmetry is much larger than the orbital velocity skewness and results in skewed orbital accelerations (Elgar et al., 1998). These time series of acceleration tend to have a maximum over the sandbar that moves shoreward with the bar, indicating some kind of feedback between them. It's been hypothesised that fluid acceleration temporarily increases the amount of sediment in motion. As a result, the temporal coincidence of strong accelerations with onshore directed orbital velocities could result in shoreward transport (Elgar et al., 2001).

Details about the unsteady bed shear stress and its phase relation to the velocity signal in the water column become more important too (Hoefel and Elgar, 2003). Waves carry a vertical flux of momentum into the WBL that forces a shoreward mean Eulerian streaming flow near the bed (Longuet-Higgins, 1953), that is maximum over the sand bar (Trowbridge and Young, 1989). This streaming can be modified and even reversed by the covariance between eddy viscosity and velocity shear that occurs under non sinusoidal waves (Trowbridge and Madsen, 1984). Existing simulations based on boundary layer model predictions of bed shear stress have been successful in predicting onshore bar migration (Henderson et al., 2004), but have not often been tested in erosional conditions due to inaccuracies in model representations of undertow.

Stokes drift can induce shoreward sediment transport (van Hardenberg et al., 1991; Deigaard et al., 1999), and has a maximum over the sandbar under moderately energetic waves. The Stokes drift is the same order of magnitude as the WBL streaming or, as the cross-shore mass balance indicates, as the undertow (Henderson et al., 2004).

This paper will report a test of a coupled Boussinesq/bottom boundary layer model for cross-shore transport, applied in accretional wave conditions. The model calculations will be conducted in predictive mode in order to assess model skill in performing short term assessments of beach profile evolution for single storm events.

CROSSTEX EXPERIMENT

A new data set was obtained during summer 2005 as part of the CROSSTEX

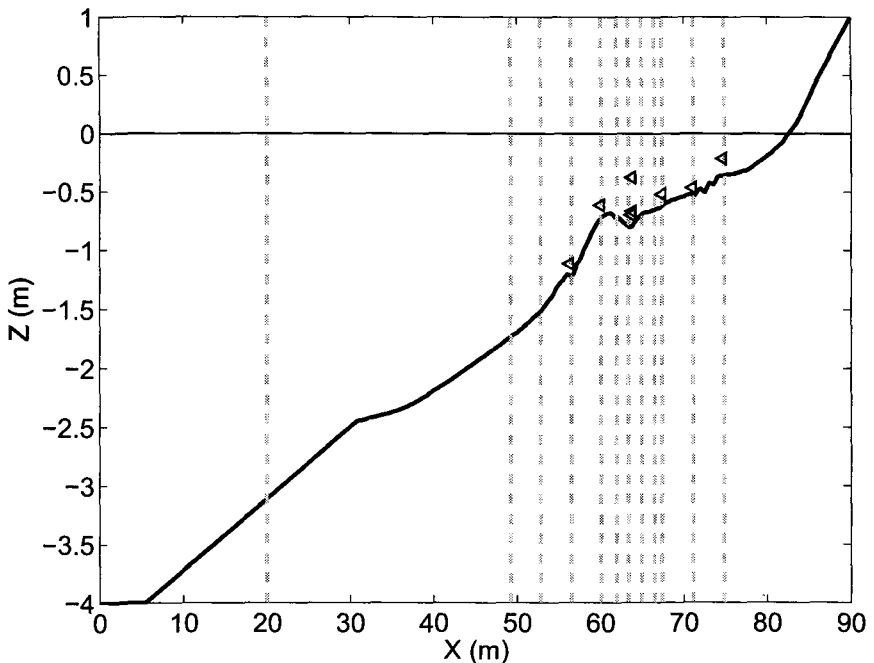


FIG. 1. Sectional elevation of the LWF and instrument locations. (Vertical grey dashed lines, wave gauges; black triangles, velocimeter locations)

experiment, conducted in the large wave flume facility at Oregon State University. Irregular waves were generated with a hinged-type, hydraulic ram wave maker, using the TMA spectrum (Bouws et al, 1985). Typical data runs lasted 20 minutes, of which 15 minutes were used for active wave generation. 0.2mm mean diameter natural sand from Oregon beaches was placed to build a 1/20 slope beach into the 104m long, 3.7m wide and 4.6m deep basin (figure 1). 13 wave gauges, located on the East wall, recorded free surface elevation from the proximity of wave maker up to the inner surf zone. A dense array of Acoustic Doppler Velocimeters recorded velocity time series at variable locations of interest. Beach profiles were typically measured after each data run, using a carriage-mounted MTA system. General details about the experiment and profiles may be found in Maddux et al. (2006).

Two major migration events were studied during the experiment. From 08/23/2005 to 08/25/2005, erosional conditions led to offshore transport and formation of a pronounced bar. Bar crest location shifted from $x = 64m$ to $x = 61m$, filling the shore side bar trough (Figure 2). Wave conditions corresponded to a TMA spectrum with $H_s = 0.60m$, $T_{peak} = 4s$, and $\gamma = 2$.

From 08/26/2005 to 09/02/2005, accretional wave conditions led to an onshore

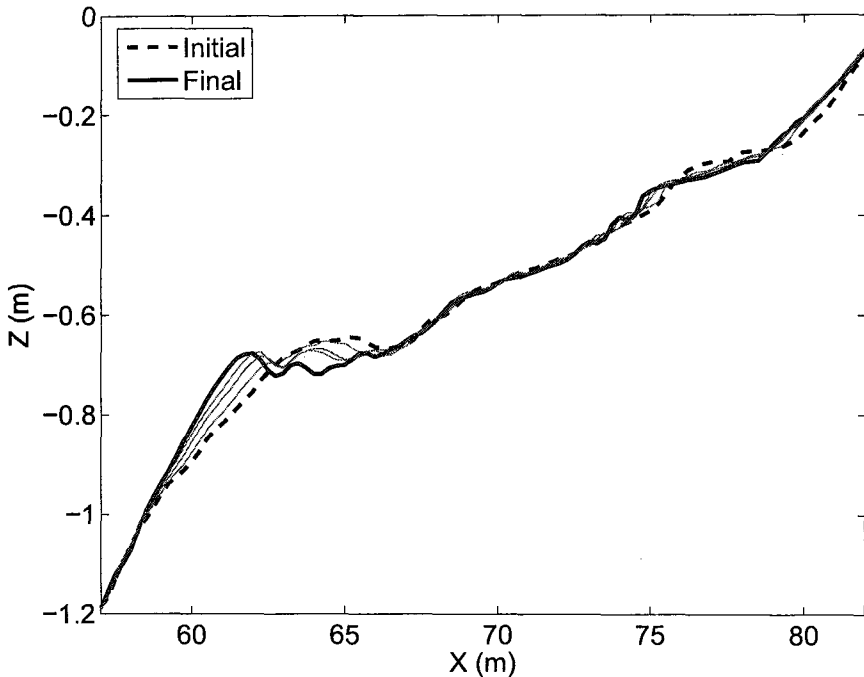


FIG. 2. Measured profile evolution, erosional case 08/23/05-08/25/05.

migration event. A wave height $H_s = 0.30m$, peak period $T_{peak} = 8s$ and a $\gamma=10$ were used. As a result, the sandbar crest migrated from location $x = 61m$ to $x = 67.5m$. (Figure 3).

MODEL

The model used here is an extension of the coupled Boussinesq/boundary layer model described by Long et al. (2004). A fully nonlinear Boussinesq model is used to predict the velocity above the bed resulting from a shoaling wave train. Fluid velocity is split into an irrotational wave component u_w , and a rotational component u_r ,

$$u = u_w + u_r \quad (1)$$

The vertical component of rotational flow is assumed negligible relative to the irrotational component, giving

$$w = w_w \quad (2)$$

Boussinesq equations for the irrotational component are derived from the Euler equations as shown in Nwogu (1993). We restrict our attention here to flows in

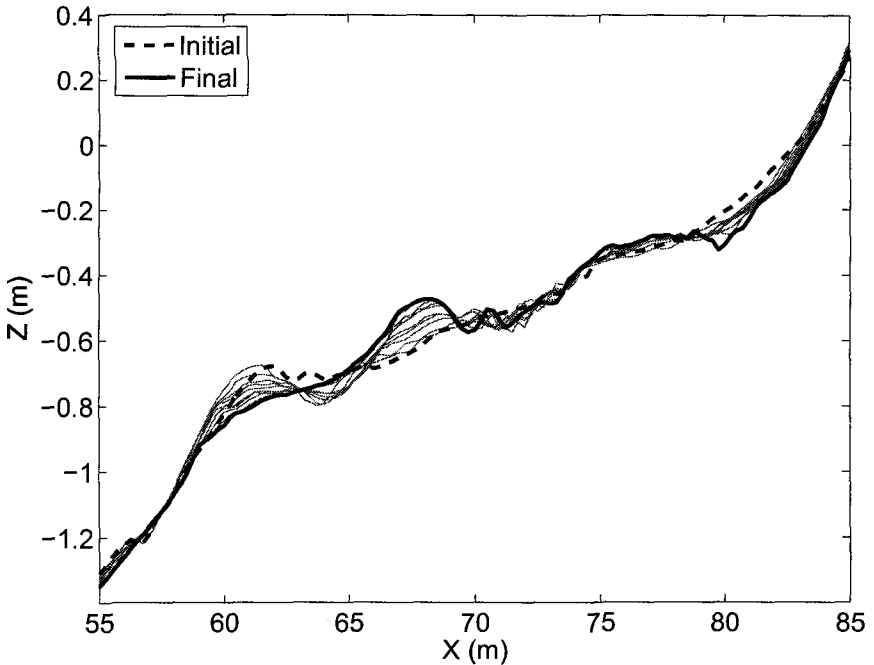


FIG. 3. Measured profile evolution, accretional case, 08/26/05-09/02/2005.

one horizontal direction x , and hence discussions of vertical vorticity dynamics, as in Chen et al (2003), are not relevant to the present study.

The model of Long et al (2004) lacked a reasonable description of broken wave roller volume flux, and hence undertow was typically underpredicted. As a result, the model had less capability for predicting undertow-dominated erosional events, usually the easier case for wave-averaged process models. Long et al (2006a) have derived a revised model incorporating wave roller flux explicitly.

The new set of equations result from momentum balance for fluid particles on an arbitrary and moving level. The mass conservation equation is given by

$$\frac{\partial \eta}{\partial t} + \frac{\partial M_w}{\partial x} + \frac{\partial M_r}{\partial x} = 0 \tag{3}$$

Where M_w (M_r) is the flux due to irrotational (rotational) flow u_w (u_r), defined by

$$M_w \equiv \int_{-h}^{\delta \eta} u_w dz \tag{4}$$

$$M_r \equiv \int_{-h}^{\delta \eta} u_r dz \tag{5}$$

The horizontal momentum equation is given by

$$\begin{aligned} & \frac{\partial M_r}{\partial t} + \frac{\partial M_w}{\partial t} + \frac{\partial}{\partial x} \left[\frac{M_r M_w}{H} + \frac{CCr^2 - M_{wr} M_{wr}}{r} \right] \\ & + \frac{\partial}{\partial x} \left[\frac{H^2}{2} - H^2 [F_{23t} + (\frac{2H}{3} - h) F_{22t}] + \tilde{u} [F_{23} + (\frac{2H}{3} - h) F_{22}] \right] \\ & - \frac{\partial h}{\partial x} \left[H - 2H \{ [F_{23t} + (\frac{H}{2} - h) F_{22}] + \tilde{u} [F_{23} + (\frac{H}{2} - h) F_{22}] \} \right] = 0 \end{aligned} \quad (6)$$

where F_{ij} are expressions involving the gradient and divergence of several quantities (Long et al, 2006a), C is the wave phase speed, r is the roller thickness and M_{wr} is the wave velocity contribution to the flux in the roller, given by

$$M_{wr} \equiv \int_{-h}^{\eta-r\eta} u_r dz \quad (7)$$

Long et al (2006a) have verified that the roller model reproduces depth-averaged undertow values when compared to several test cases. However, the uniform-over-depth undertow structure underpredicts near bottom velocities, resulting offshore transport underestimation in erosional situations. The Long et al (2006a) model is used here to examine the accretional case illustrated in Figure 2, where the influence of undertow is of less importance.

Model predicted velocities are then used to drive one-dimensional vertical boundary layer calculations at a horizontal resolution which is somewhat less than grid for the Boussinesq calculation. The time-dependent boundary layer equations are based on continuity equation and approximations from Reynolds-Averaged Navier-Stokes equation as in Hsu and Hanes (2004). Turbulent Reynolds stress are parameterized in terms of a turbulent eddy viscosity given by mixing length theory or $k-\epsilon$ model (Hsu and Hanes, 2004).

After estimating the instantaneous bed shear stress, sediment transport is estimated using the Meyer-Peter Muller formula. The total transport rate is given by

$$\Psi = \frac{q_{tot}}{\sqrt{d(s-1)gd}} \quad (8)$$

The normalized transport rate can be expressed as

$$\Psi = A(\theta_c - \theta)^b \quad (9)$$

with $A = 11$, $b = 1.65$ and θ_c the threshold value for initiation of transport. The Shields parameter is

$$\theta = \frac{\tau_b}{\sqrt{(\rho_s - \rho)gd}} \quad (10)$$

Instantaneous transport is accumulated over several wave periods. Bed level changes are then given by the equation for sediment volume concentration

$$\frac{\partial z_b}{\partial t} = \frac{-1}{1 - n_p} \cdot \nabla q \quad (11)$$

where z_b is the bed level elevation, n_p is the bed porosity, and q is the total volumetric sediment transport rate. Equation (11) is solved using an Euler-WENO scheme described in Long et al (2006b).

MODEL SIMULATIONS

The accretional event illustrated in Figure 3 spans a period of 50 20-minute runs with steady input wave conditions. Model simulations spanning this period were conducted in predictive mode, using only the initial bathymetry and incident waves as input. The real domain is implemented in the numerical model minimizing the grid space as much as the numerical stability allows. Measured time series at location $x = 20m$ and water depth $h = 3.1m$ is used as wave maker input in the model. A wave maker region occupies the region between $x = 4m$ to $x = 36m$. Finally, a sponge layer is located seawards, the wave maker in order to absorb reflected waves from the beach.

Attempts to tune the hydrodynamic model have been made. First, wave breaking model was optimized to improve the wave height distribution. Also, the sponge layer length and its efficiency were tuned to suppress spurious low frequency motions. With respect to the sediment transport model, transport efficiency was modified to certain extent.

Model simulations successfully predict first and second order hydrodynamic quantities such as free surface elevation and wave height distribution. An example comparison of measured and modeled surface elevation is shown in Figure 4.

First order statistical quantities such as the H_{mo} distribution and associated wave period are shown in Figure 5. Good agreement is achieved between measured and predicted heights and periods at the wave gauge locations. However, small discrepancies appear close to the shoreline due to model inaccuracies. Free surface spectral density computations reveals the model recovers most of the energy in the peak frequency (Figure 6). Again, some of the low frequency motion is being underpredicted.

Figure 7 shows the initial profile along with final measured and modeled profiles after 50 runs. The modeled bar moves landward, but only by a small amount, lagging far behind the motion of the measured bar feature. This result indicates that further adjustments are needed in hydrodynamic and sediment transport relations in the model. In particular, the tendency for the bar to remain closer to the initial position indicated that breaking events over the bar crest are probably too frequent during the model simulations. We are presently trying to assess this hypothesis using video data collected during the experiment.

During initial testing, the model exhibited the spurious growth of a pronounced bar feature close to shore, resulting from rapid erosion of the beach face in the region of the swash zone. This result was apparently due to the presence of unnaturally large reflections from the steep shoreface, due to non-physical behavior caused by the thin-film shoreline boundary treatment (Long et al, 2006a). The resulting bar caused by rapid shoreline erosion accumulated at nodal positions of the cross-shore standing wave pattern associated with sieching modes in

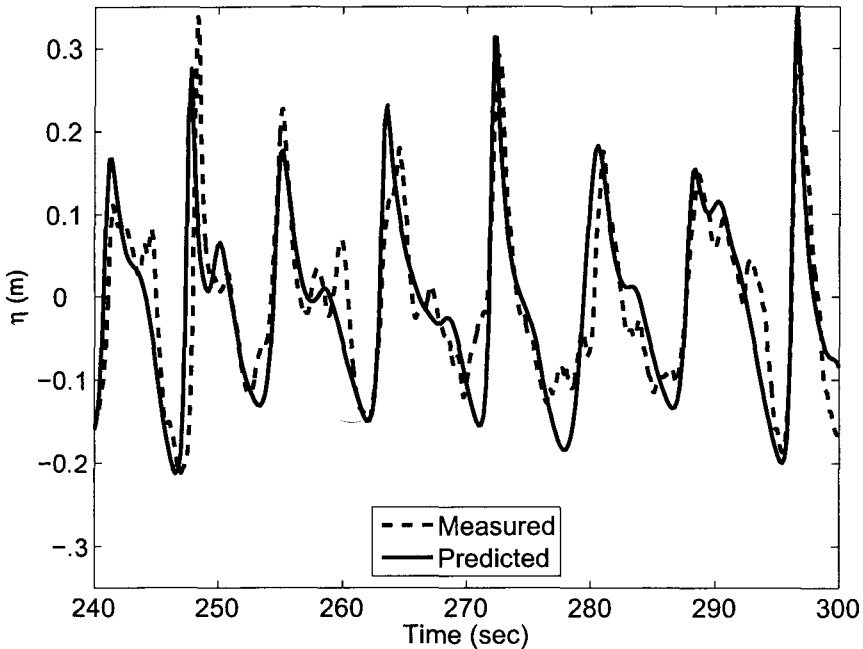


FIG. 4. Free surface displacement. Wave Gauge 5 ($x=60.1$ m). Day 08/26/2005. Run06.

the numerical model. To suppress this behavior, transport in the swash was subsequently suppressed using a smooth roll-off of computed transport rate close to and beyond the still water shoreline. Tests were conducted verifying that mass conservation is satisfied for the sand volume.

The model performance can be quantitatively assessed by means of the skill test (Gallagher et al., 1998). Skill S is defined as

$$S = 1 - \frac{E_{rms}}{\Delta_{rms}} \quad (12)$$

where E_{rms} is the root mean square (RMS) change between predicted and observed profiles, and Δ_{rms} is the RMS change between initial and final observed profiles. Following Gallagher et al. (1998), $S = 1$ when the errors vanish. When the errors are as large as the observed changes, $S = 0$, meaning the model prediction is as good as if the final and initial profiles were the same. Finally, a negative skill would appear if the errors were larger than the observed changes.

Values of S are available starting at Run04, for which another measured bathymetry to compare with is available for first time. From a negative value of $S = -0.9$, and throughout the 50 runs, S exhibits a clear slow tendency to improve reaching positive values after just ten executions (Figure 8). This initial improvement is due to the dominant influence of erosion the initial bar.

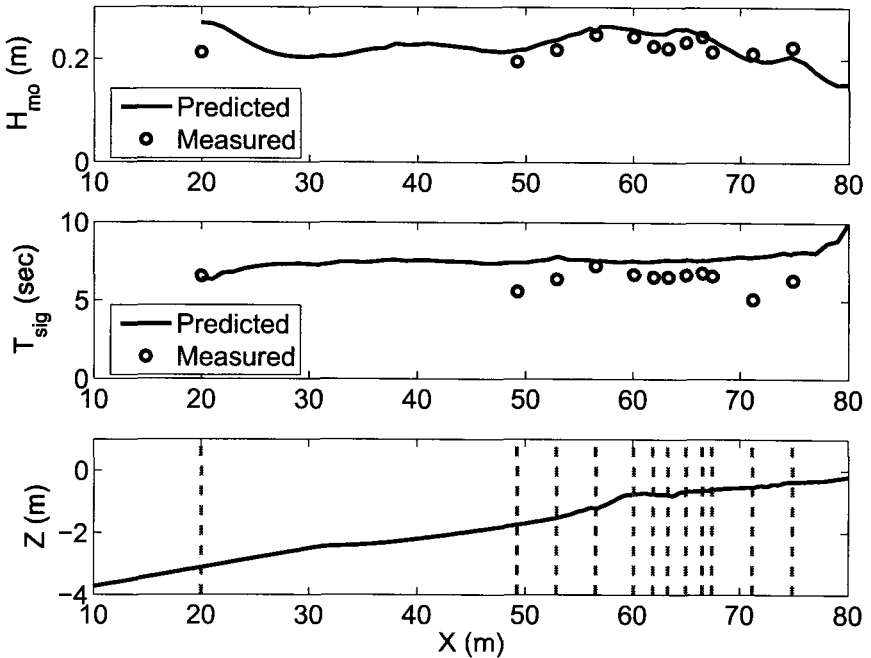


FIG. 5. Wave height distribution and associated periods. Day 08/26/2005. Run06.

However, since the model-simulated bar does not move landward by the correct amount, overall error in profile change grows rapidly, leading to a drop in S back to negative values.

DISCUSSION

Large scale laboratory experiments allow for better environmental control of wave conditions and elimination of effects associated with the longshore dimension. However, phenomena like seiching, or limitations such as steep beach slope and the resulting greater proximity of the shoreline to the surfzone when compared to real beaches, can cause difficulties both in numerical simulations and in interpretation of laboratory results in comparison to field observations. Our work here has shown that further attention is needed to the details of shoreline reflection, swashzone sediment transport, and details of breaking wave simulation over nearshore bar crests. Errors in model behavior, specially when strong reflection takes place, have a cumulative effect over the consecutive 50 simulations, and tend to drive bathymetry evolution away from the observed pattern. The add hoc treatment of the swash zone has proven to provide valid morphological predictions, but still requires a more physically meaningful treatment. As expected, the model performance on onshore sandbar migration has

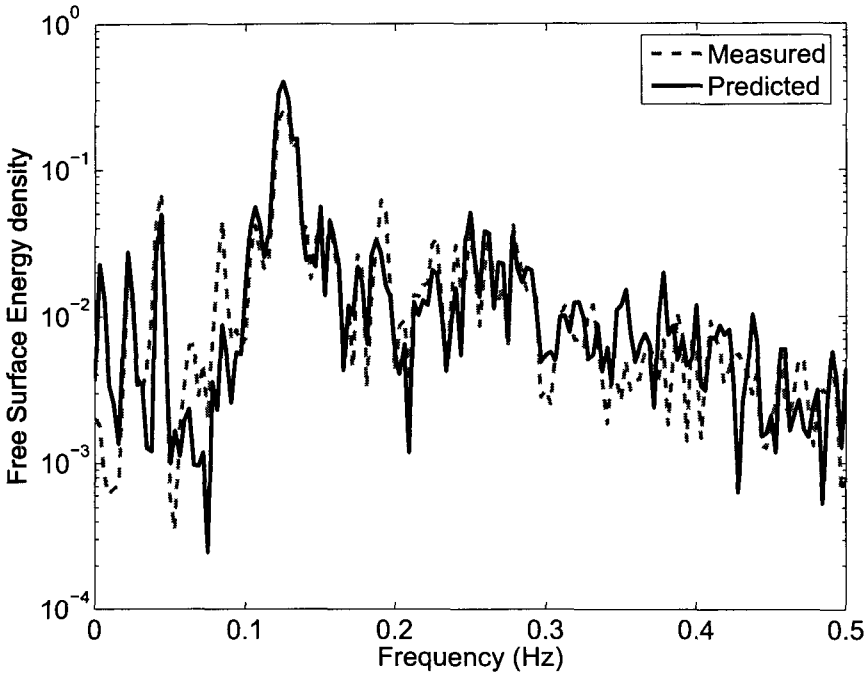


FIG. 6. Free surface density spectrum with 12 degrees of freedom, $\Delta f = 1/200\text{sec}$. Wave gauge 5 (on top of the bar crest) Day 08/26/2005. Run06.

shown a strong dependence on the predicted hydrodynamics. Accurate estimation of the flow field is therefore essential in order to improve the sediment transport estimations. Thus, some progress must be made in various aspects of the wave hydrodynamics before improved morphology predictions can be expected.

ACKNOWLEDGMENTS

This work was supported by the National Science Foundation, Physical Oceanography Program, Grant OCE-0351297. We wish to thank the faculty and staff of the O. H. Hinsdale Wave Research Laboratory for their time and support during the experimental phase of CROSSTEX. The O.H. Hinsdale Wave Research laboratory is partially supported by the George E. Brown Jr. Network for Earthquake Engineering Simulation (NEES) Consortium Incorporated contract OMSA v.3.1 through the National Science Foundation Cooperative Agreement CMS-0402490. Instrumentation used in this project was purchased under NSF-0429219.

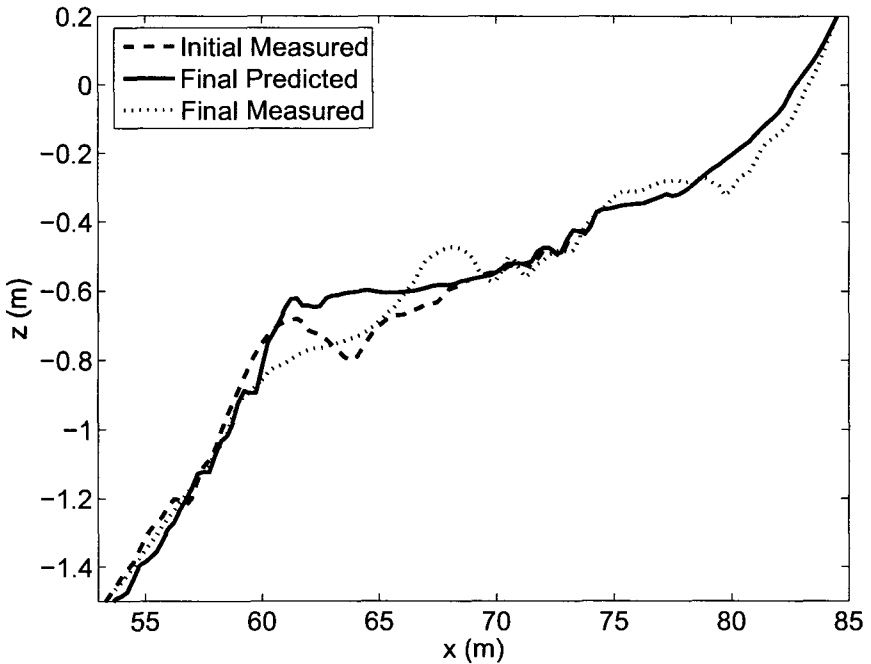


FIG. 7. Predicted profile evolution during accretional bar migration period.

REFERENCES

- Aubrey, D.G., 1979. Seasonal patterns of onshore/offshore sediment movement, *J. Geophys. Res.*, 84, 6347–6354.
- Bagnold, R.A., 1956. Flow of cohesionless grains in fluids, *Phil. Trans. Roy. Soc. London*, 249, 235–297.
- Bagnold, R.A., 1966. An approach to the sediment transport problem from general physics, *U.S. Geol. Surv. Prof. Pap.*, 422-I, Reston, Va.
- Bailard, J.A., 1981. An energetics total load sediment transport model for a plane sloping beach, *J. Geophys. Res.*, 86, 10,938–10,964.
- Bouws, E., Gunter, H., Rosenthal, W. and Vincent, C.I. 1985. Similarity of the wave pectrum in finite depth water: 1. spectral form, *J. Geophys. Res.*, 90,975–986.
- Bowen, A.J., 1981. Simple models of nearshore sedimentation: Beach profiles and longshore bars, *Coastline Can.*, 80-10,1–11.
- Chen, Q., Kirby, J. T., Dalrymple, R. A., Shi, F. and Thornton, E. B., 2003. Boussinesq modeling of longshore currents *J. Geophys. Res.*, 108(C11), 3362, doi:10.1029/2002JC001308.
- Dally, W.R. And Dean, R.G., 1984. Suspended sediment transport and beach

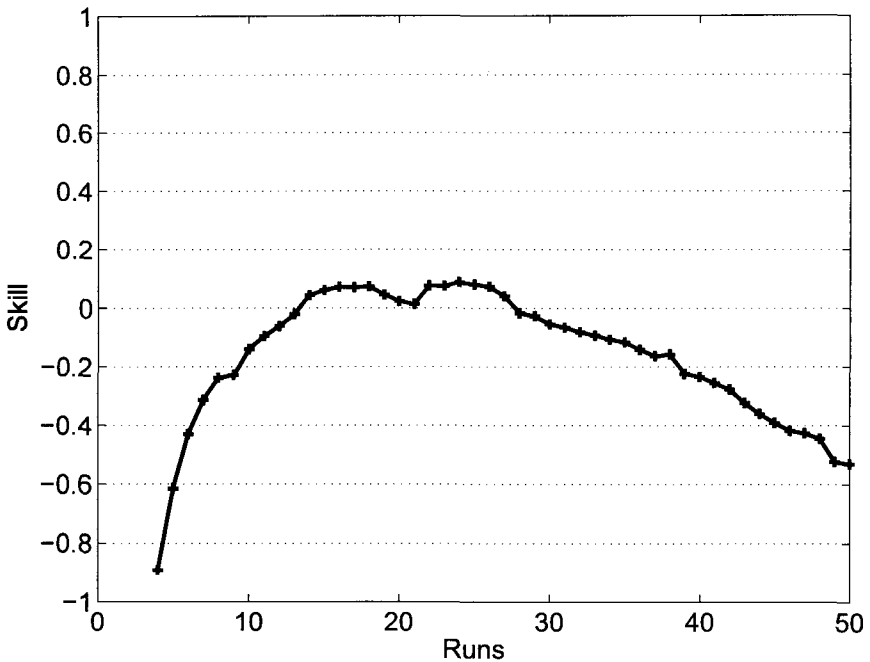


FIG. 8. Skill values S from run 4 to 50.

profile evolution, *J. Waterw., Port, Coastal Ocean Div. Am. Soc. of Civil Eng.*, 110, 15–33.

Deigaard, R., J.B. Jakobsen and J. Fredsoe, 1999. Net sediment transport under wave groups and bound long waves, *J. Geophys. Res.*, 104, 13,559–13,575.

Elgar, S., R.T. Guza and M. Freilich, 1988. Eulerian measurements of horizontal accelerations in shoaling gravity waves, *J. Geophys. Res.*, 93, 9261–9269.

Elgar, S., E.L. Gallagher and R. Guza, 2001. Nearshore sandbar migration, *J. Geophys. Res.*, 106, 11,623–11,627.

Gallagher, E.L., S. Elgar, and R. Guza, 1998. Observations of sand bar evolution on a natural beach, *J. Geophys. Res.*, 103, 3203–3215.

Haines, J.W. and A.H. Sallenger, 1994. Vertical structure of mean cross-shore currents across a barred surf zone, *J. Geophys. Res.*, 99, 14223–14242.

Henderson, M.H., J.S. Allen and P.A. Newberger, 2004. Nearshore sandbar migration predicted by an eddy-diffusive boundary layer model, *J. Geophys. Res.*, 109, C06024, doi:10.1029/2003JC002137.

Hoefel, F. and S. Elgar, 2003. Wave induced sediment transport and sandbar migration, *Science*, 299, 1885–1887.

Hsu, T-J. and D.M. Hanes, 2004. The effect of wave shape on sheet flow sediment

- transport, *J. Geophys. Res.*, 109, C06025, doi: 10.1029/2003JC002075.
- Lippman, T.C., E.B. Thornton and A.J.H.M. Reniers, 1996. Wave stress and longshore current on barred profiles, *Proc. Coastal Dynamics '95*, Am. Soc. of Civil Eng., 401–412, New York.
- Long, W., Hsu, T.-J. and Kirby, J. T., 2004. Modeling cross-shore sediment transport processes with a time domain Boussinesq model, *Proc. 29th Int. Conf. Coastal Eng.*, Lisbon, September, 1874–1886.
- Long, W., Kirby, J. T. and Hsu, T.-J., 2006a. Cross shore sandbar migration predicted by a time domain Boussinesq model incorporating undertow, *Proc. 30th Int. Conf. Coastal Eng., San Diego*, in press.
- Long, W., Kirby, J. T. and Shao, Z., 2006b. Numerical schemes for bed level updating in sediment transport, submitted to *Coastal Engineering*.
- Longuet-Higgins, M. S., 1953. Mass transport in water waves, *Phil. Trans. Roy. Soc. London A*, 245, 535–581.
- Maddux, T.B., Cowen, E.A., Foster, D.L., Haller, M.C. and Stanton, T.P., 2006. The Cross Shore sediment transport experiment (CROSSTEX), *Proc. 30th Intl. Conf. Coastal Eng., San Diego*, in press.
- Nwogu, O., 1993. Alternative Form of Boussinesq Equations for Nearshore Wave Propagation, *J. Waterway, Port, Coastal and Ocean Engineering, ASCE*, 119(6), 618–638.
- Sallenger, A.H. and P.A. Howd, 1989. Nearshore bars and the break-point hypothesis, *Coastal Eng.*, 12, 301–13.
- Thornton, E.B. and W. Birkemeier, 1996. Bar/trough generation on a natural beach, *J. Geophys. Res.*, 101(C5), 12,097–12,110.
- Trowbridge, J. and D. Young, 1989. Sand transport by unbroken water waves under sheet flow conditions, *J. Geophys. Res.*, 94, 10,971–10,991.
- Trowbridge, J. and O. Madsen, 1984. Turbulent wave boundary layers: Second order theory and mass transport, *J. Geophys. Res.*, 89, 7999–8007.
- van Hardenberg, B., A. Hay, Y. Sheng and A. Bowen, 1991. Field measurements of the vertical structure suspended sediment, *Proc. Coastal Dynamics '91*, Am. Soc. of Civil Eng., 300–312.